

QUASI-PERIODICITY VERSUS HYPERCHAOS OF TRIPLE PHYSICAL PENDULUM WITH IMPACTS

Jan Awrejcewicz and Grzegorz Kudra

Technical University of Lodz

Division of Automatics and Biomechanics (K-16)

1/15 Stefanowskiego St.

90-924

Lodz

Poland

awrejcew@ck-sg.p.lodz.pl and grekudra@ck-sg.p.lodz.pl

ABSTRACT

In this work the triple pendulum with damping, external forcing and with impacts is investigated. The extension of a coefficient restitution rule and a special transition condition rule for perturbation (linearized system in the Lyapunov exponents algorithm) in each discontinuity point are applied. Periodic, quasi-periodic, chaotic and hyperchaotic motions are observed using Poincaré maps and bifurcational diagrams, which are verified by the Lyapunov exponents. In addition basins of attraction of some coexisting regular and irregular attractors are illustrated and discussed.

KEYWORDS: triple pendulum, quasi-periodicity, chaos, Poincaré map, coexisting solutions, bifurcation.

INTRODUCTION

A pendulum plays a very important role in mechanics since many interesting non-linear dynamical behaviour can be illustrated and analysed using this system (Acheson and Mullin, 1993; Bishop and Clifford, 1996; Skeldon 1994; Yagasaki 1994). Even simple pendulum externally excited can exhibit periodic, quasi-periodic and chaotic dynamics. It is obvious that coupled pendulums with obstacles can serve as a model even for a very complicated behaviour including that of energy pumped to the model, a various amount of resonances, jumps between different system states, various continuous and discontinuous bifurcations, etc.

INVESTIGATED PENDULUM AND GOVERNING EQUATIONS WITHOUT IMPACTS

Three joined physical pendulums in the global co-ordinate system x, y, z (with origin in point O_1) are presented in Figure 1. A local co-ordinate system x_{Cl}, y_{Cl}, z_{Cl} formed by

principal central co-ordinate axes is attached to each of the i -th link. It is assumed that the links are absolute stiff bodies moving in a vacuum and coupled by viscous damping with the coefficients \bar{c}_i ($i = 1,2,3$). The first body is excited by harmonic action $\bar{q}_1 \cos \bar{\omega}_1 \tau$, where τ denotes time. In addition it has been assumed, that :

- the mass centres of the links lie on the lines including the joints O_i ;
- one of the principal central axes of each link (z_{ci}) is perpendicular to a movement plane of the pendulum ;
- one of the principal central axes of each link (y_{ci}) overlaps with a line including the pendulum axes O_i .

The introduced assumptions result in getting symmetric system.

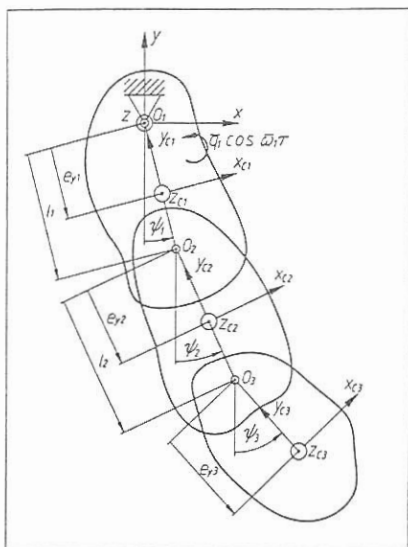


Figure 1. The investigated triple pendulum.

The governing differential equations of systems without impacts have the following non-dimensional form

$$M \cdot \ddot{\psi} + B \cdot \dot{\psi}^2 + C \cdot \psi + D = F, \quad (1)$$

where

$$\ddot{\psi} = \begin{Bmatrix} \ddot{\psi}_1 \\ \ddot{\psi}_2 \\ \ddot{\psi}_3 \end{Bmatrix}, \quad \dot{\psi}^2 = \begin{Bmatrix} \dot{\psi}_1^2 \\ \dot{\psi}_2^2 \\ \dot{\psi}_3^2 \end{Bmatrix}, \quad \dot{\psi} = \begin{Bmatrix} \dot{\psi}_1 \\ \dot{\psi}_2 \\ \dot{\psi}_3 \end{Bmatrix},$$

$$M = \begin{bmatrix} 1 & v_{12} \cos(\psi_1 - \psi_2) & v_{13} \cos(\psi_1 - \psi_3) \\ v_{12} \cos(\psi_1 - \psi_2) & \beta_2 & v_{23} \cos(\psi_2 - \psi_3) \\ v_{13} \cos(\psi_1 - \psi_3) & v_{23} \cos(\psi_2 - \psi_3) & \beta_3 \end{bmatrix}, \quad (2)$$

$$B = \begin{bmatrix} 0 & v_{12} \sin(\psi_1 - \psi_2) & v_{13} \sin(\psi_1 - \psi_3) \\ -v_{12} \sin(\psi_1 - \psi_2) & 0 & v_{23} \sin(\psi_2 - \psi_3) \\ -v_{13} \sin(\psi_1 - \psi_3) & -v_{23} \sin(\psi_2 - \psi_3) & 0 \end{bmatrix},$$

$$C = \begin{bmatrix} c_1 + c_2 & -c_2 & 0 \\ -c_2 & c_2 + c_3 & -c_3 \\ 0 & -c_3 & c_3 \end{bmatrix}, \quad D = \begin{Bmatrix} \sin \psi_1 \\ \sin \psi_2 \\ \sin \psi_3 \end{Bmatrix}, \quad F = \begin{Bmatrix} q_1 \cos \omega_1 t \\ 0 \\ 0 \end{Bmatrix}.$$

The relations between dimensional and non-dimensional parameters are as follows

$$\beta_2 = \frac{B_2}{B_1}, \quad \beta_3 = \frac{B_3}{B_1}, \quad \mu_2 = \frac{M_2}{M_1}, \quad \mu_3 = \frac{M_3}{M_1}, \quad (3)$$

$$\kappa_1 = \frac{K_1}{B_1}, \quad \kappa_2 = \frac{K_2}{B_1}, \quad \kappa_3 = \frac{K_3}{B_1}, \quad v_{12} = \frac{N_{12}}{B_1}, \quad v_{13} = \frac{N_{13}}{B_1}, \quad v_{23} = \frac{N_{23}}{B_1},$$

$$c_1 = 2 \frac{\bar{c}_1}{\sqrt{M_1 B_1}}, \quad c_2 = 2 \frac{\bar{c}_2}{\sqrt{M_1 B_1}}, \quad c_3 = 2 \frac{\bar{c}_3}{\sqrt{M_1 B_1}}, \quad (4)$$

and

$$q_1 = \frac{\bar{q}_1}{M_1}, \quad (5)$$

where

$$\begin{aligned}
 B_1 &= J_{z_1} + e_{y_1}^2 m_1 + l_1^2 (m_1 + m_2), \quad B_2 = J_{z_2} + e_{y_2}^2 m_2 + l_2^2 m_3, \quad B_3 = J_{z_3} + e_{y_3}^2 m_3, \\
 M_1 &= m_1 g e_{y_1} + (m_2 + m_3) g l_1, \quad M_2 = m_2 g e_{y_2} + m_3 g l_2, \quad M_3 = m_3 g e_{y_3}, \\
 K_1 &= J_{x_1} - J_{y_1} + e_{y_1}^2 m_1 + l_1^2 (m_1 + m_2), \quad K_2 = J_{x_2} - J_{y_2} + e_{y_2}^2 m_2 + l_2^2 m_3, \\
 K_3 &= J_{x_3} - J_{y_3} + e_{y_3}^2 m_3, \\
 N_{12} &= m_2 e_{y_2} l_1 + m_3 l_1 l_2, \quad N_{13} = m_3 e_{y_3} l_1, \quad N_{23} = m_3 e_{y_3} l_2.
 \end{aligned} \tag{6}$$

Above $J_{x_i}, J_{y_i}, J_{z_i}$ ($i=1,2,3$) denote the appropriate principal inertia momenta and m_i ($i=1,2,3$) denote the appropriate masses. The relations between real and non-dimensional time has the form

$$t = \alpha_1 \tau, \tag{7}$$

$$\text{where: } \alpha_1^2 = \frac{M_1}{B_1}.$$

The relations between derivatives with respect to real and non-dimensional time have the forms

$$\frac{d\psi_i}{d\tau} = \alpha_1 \frac{d\psi_i}{dt} = \alpha_1 \dot{\psi}_i, \quad \frac{d^2\psi_i}{d\tau^2} = \alpha_1^2 \frac{d^2\psi_i}{dt^2} = \alpha_1^2 \ddot{\psi}_i, \quad i = 1,2,3 \tag{8}$$

$$\bar{\omega}_i = \alpha_1 \omega_i.$$

Observe that the introduction of the non-dimensional form of the governing equations has decreased the number of parameters (from 23 real parameters to 16 non-dimensional ones). Moreover the non-dimensional equations may govern not only our system of triple pendulum, but also others similar like systems (Bayly and Virgin, 1992; Heng et al. 1994).

INTRODUCTION OF THE OBSTACLES TO THE SYSTEM

When in the investigated system the physical rigid obstacles appear, the governing equations can be written as follows:

$$\begin{aligned}
 M \cdot \ddot{\psi} + B \cdot \dot{\psi}^2 + C \cdot \dot{\psi} + D = F, \\
 h_i(\psi) \geq 0, \quad (i = 1, \dots, n),
 \end{aligned} \tag{9}$$

where the inequality $h_i(\psi) \geq 0$ represents an unilateral constraint that is imposed on the position of the system, and n is the number of constraints (obstacles).

In (Brogliato, 1999), the extension of Newton's rule (restitution coefficient rule) to more than one degree-of-freedom systems is considered. It is shown that for a Lagrangian system with generalized coordinates ψ , with a frictionless unilateral constraint $h_i(\psi) \geq 0$, the only

possible rule is to apply Newton's restitution rule to the component of $\dot{\psi}$ along $\nabla_{\psi} h_i(\psi)$, which reads:

$$n_{\psi}^T \cdot \dot{\psi}^* = -e n_{\psi}^T \cdot \dot{\psi}^-, \quad (10)$$

($n_{\psi} = \frac{\nabla_{\psi} h_i(\psi)}{\|\nabla_{\psi} h_i(\psi)\|}$ is the unitary normal vector, and e is the restitution coefficient), and then to calculate the remaining postimpact velocity components using the shock dynamics equations

$$t_{\psi,1}^T \cdot M(\psi) \cdot \begin{Bmatrix} \dot{\psi}_1^+ - \dot{\psi}_1^- \\ \dot{\psi}_2^+ - \dot{\psi}_2^- \\ \dot{\psi}_3^+ - \dot{\psi}_3^- \end{Bmatrix} = 0, \quad t_{\psi,2}^T \cdot M(\psi) \cdot \begin{Bmatrix} \dot{\psi}_1^+ - \dot{\psi}_1^- \\ \dot{\psi}_2^+ - \dot{\psi}_2^- \\ \dot{\psi}_3^+ - \dot{\psi}_3^- \end{Bmatrix} = 0, \quad (11)$$

where $t_{\psi,1}$ and $t_{\psi,2}$ are the tangent unitary vectors chosen as mutually independent, i.e. $t_{\psi,1}^T \cdot \nabla_{\psi} h_i(\psi) = 0$, $t_{\psi,2}^T \cdot \nabla_{\psi} h_i(\psi) = 0$ and $t_{\psi,1}^T \cdot t_{\psi,2} = 0$.

NUMERICAL EXAMPLES

A special simple case of the introduced system of coupled physical pendulums will be further analysed. We consider only three identical rods with damping, external excitation q_1 and with the obstacle in the form of horizontal wall (Figure 2).

The physical obstacle can be expressed in the following non-dimensional form

$$\begin{aligned} h_1(\psi) &= \eta - \cos\psi_1 \geq 0, \\ h_2(\psi) &= \eta - (\cos\psi_1 + \lambda_2 \cos\psi_2) \geq 0, \\ h_3(\psi) &= \eta - (\cos\psi_1 + \lambda_2 \cos\psi_2 + \lambda_3 \cos\psi_3) \geq 0, \end{aligned} \quad (12)$$

where:

$$\lambda_2 = \frac{l_2}{l_1}, \quad \lambda_3 = \frac{l_3}{l_1}, \quad \eta = \frac{h}{l_1}, \quad (13)$$

and l_i is the real length of the i -th rod and h is the real position of the horizontal wall.

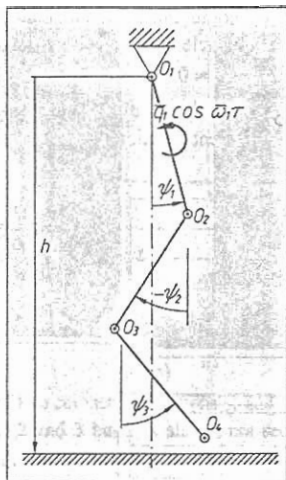


Figure 2. Three coupled rods with the obstacle.

For three identical rods we have

$$\lambda_2 = 1, \quad \lambda_3 = 1, \quad (14)$$

and others non-dimensional parameters read

$$\beta_2 = \frac{4}{7}, \quad \beta_3 = \frac{1}{7}, \quad \mu_2 = \frac{3}{5}, \quad \mu_3 = \frac{1}{5}, \quad (15)$$

$$\kappa_1 = 1, \quad \kappa_2 = \frac{4}{7}, \quad \kappa_3 = \frac{1}{7}, \quad \nu_{12} = \frac{9}{14}, \quad \nu_{13} = \frac{3}{14}, \quad \nu_{23} = \frac{3}{14}.$$

The fourth order Runge-Kutta method with detection of each point of an impact with an arbitrary precision has been used to integrate the obtained system of ordinary differential equations. In each impact point the system state has been transformed using equations (10) and (11).

The Lyapunov exponents have been computed directly from the differential equations using well known algorithm (Wolf et al., 1985). Because of discontinuities, a linearized system which represents the perturbation motion, have been transformed (Müller, 1995) in each point of a discontinuity using special rules.

We present (see Figures 3-6) some numerically obtained examples for three identical coupled rods with the physical obstacle introduced in Figure 2. The following parameters are fixed: $\eta = 2.5$, $e = 1$, $c_1 = c_2 = c_3 = 0.1$ and $\omega_1 = 1$. The q_1 parameter has been varied within the interval $(0.75, 0.7885)$ and the initial conditions of the system are varied, too. In the considered interval three different solutions have been detected, and their bifurcational histories are reported in Figure 3.

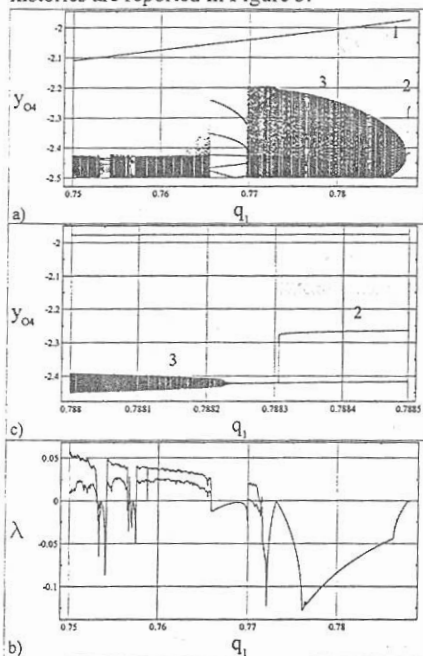


Figure 3. Bifurcational diagram for (a) $q_1 \in (0.7500, 0.7885)$ and (c) $q_1 \in (0.7880, 0.7885)$; three coexisting solutions (1, 2 and 3), where y_{04} denotes the third rod's end co-ordinate; and the corresponding two largest Lyapunov exponents (b) (except of zero exponent) corresponding to 3 solution.

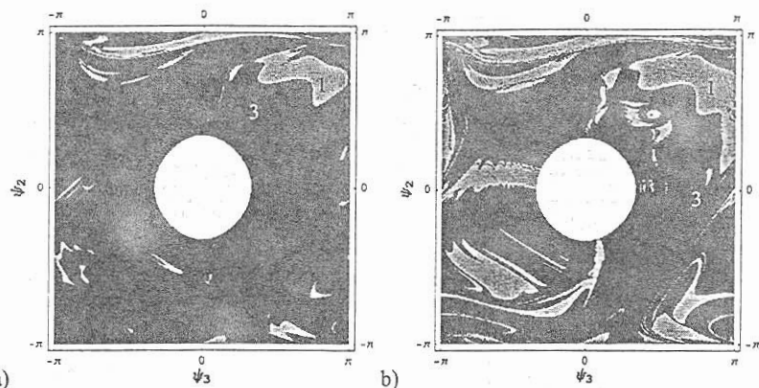
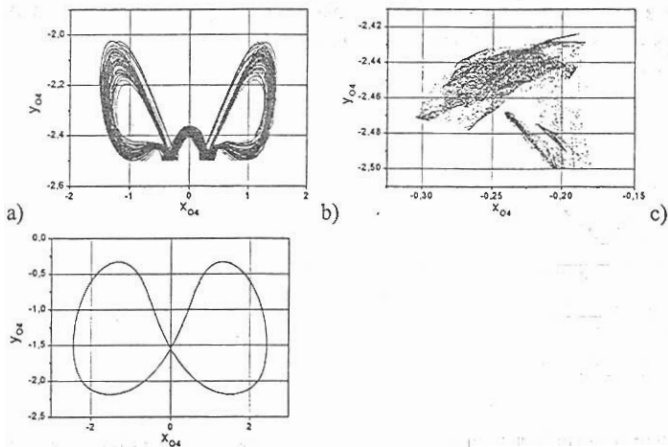


Figure 4. Basins of attraction of two coexisting solutions (1 and 3) corresponding to $q_1 = 0.75$ (a) and three coexisting solutions (1,2 and 3 but 2 is almost not seen because of very small area of existing) corresponding to $q_1 = 0.7885$ (b); the initial conditions: $\psi_1(t=0) = 0$, $\psi_2(0) \in (-\pi, \pi)$, $\psi_3(0) \in (-\pi, \pi)$, $\dot{\psi}_1(0) = \dot{\psi}_2(0) = \dot{\psi}_3(0) = 0$.



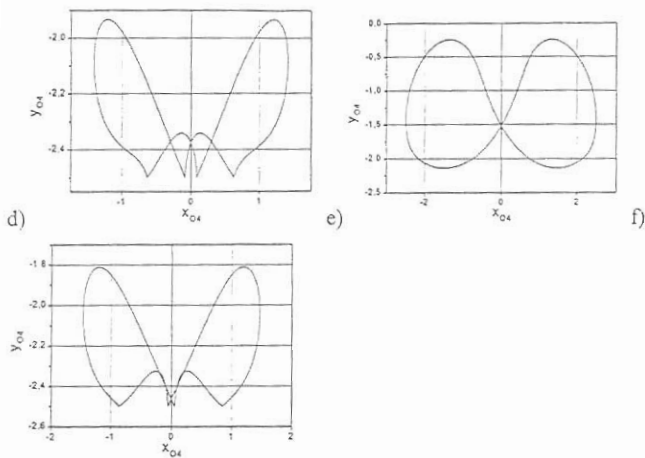


Figure 5. Solutions corresponding to $q_1 = 0.75$ (a,b,c) and $q_1 = 0.7885$ (d,e,f); a) - phase trajectory for hyperchaotic solution 3; b) - Poincaré map corresponding to (a); c) - periodic phase trajectory 1; d) - periodic phase trajectory 3; e) - phase trajectory 1; f) - phase trajectory 2.

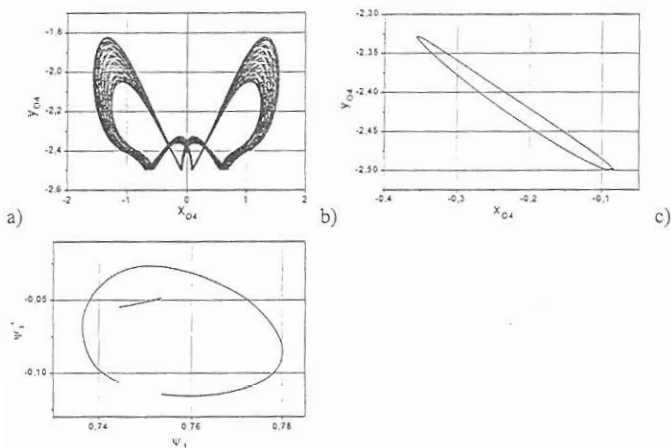


Figure 6. Quasi-periodic solution (a - phase trajectory) corresponding to $q_1 = 0.786$ (see Figure 3) with the discontinuous Poincaré section (b,c).

On Figure 4 we show the basins of attraction of these solutions for to $q_1 = 0.75$ and $q_1 = 0.7885$. The first one (1) is always being periodic one and our pendulum motion takes place without any impact. The pendulum omits the obstacle (see Figure 5c,e). The second solution (2) is also periodic but with impacts (see Figure 5f), and it vanishes for

$q_1 = 0.788106$ (see Figure 3c). The third periodic solution (3) is of most importance, since it undergoes a route to hyperchaos when q_1 is decreased. For instance for $q_1 = 0.7885$ it is periodic, whereas for $q_1 = 0.788232$ it bifurcates to quasi-periodic solution (see Figure 3b). The quasi-periodic solution for $q_1 = 0.786$ and its discontinuous Poincaré section are shown in Figure 6.

A further decrease of q_1 causes a transition to chaos for $q_1 = 0.7715$ with a short periodic window. For $q_1 = 0.7700$ again a relatively large periodic orbit domain occurs, which disappears for $q_1 = 0.7659$. Then the hyperchaos occurs, which is observed until the end of the considered interval of q_1 . The hyperchaos is interrupted by narrow periodic windows for $q_1 \in (0.7530, 0.7543)$ and $q_1 \in (0.7566, 0.7576)$, which with a high probability include also quasi-periodic and chaotic intervals. However, the latter ones are difficult distinguishable in Figure 3c.

The corresponding Lyapunov exponents are shown in Table 1.

Table 1. The Lyapunov exponents λ_i ($i = 1, \dots, 7$) for the analysed solutions.

Figure	5 a/b	5 c	5 d	5 e	5 f	6 a/b/c
λ_1	0.06	0	0	0	0	0
λ_2	0.01	-0.010	-0.0017	-0.11	-0.14	0.0000
λ_3	0	-0.010	-0.0017	-0.11	-0.28	-0.0469
λ_4	-0.67	-0.25	-0.0660	-0.26	-0.28	-0.0470
λ_5	-0.94	-0.25	-1.2626	-0.26	-0.28	-1.2963
λ_6	-1.48	-1.69	-1.7733	-1.71	-1.39	-1.6679
λ_7	-2.10	-2.40	-1.7733	-2.29	-2.56	-1.8376

CONCLUDING REMARKS

In this report we have analysed regular and irregular dynamics of triple pendulum with damping, external excitations and impacts and with physical obstacle in the form of horizontal wall. The impact law for triple pendulum in the form of generalized Newton's rule has been introduced, and other special transition conditions for disturbed motion in each impact point have been applied.

Periodic, quasi-periodic and hyperchaotic motions have been detected, discussed and illustrated. The basins of attraction for three coexisting periodic solutions have been reported, and a transition to hyperchaos has been illustrated.

REFERENCES

- Acheson, D. J. And Mullin, T. (1993). Upside down pendulums. *Nature* **366**, 215-216.
 Bishop, S.R. And Clifford, M.J. (1996). Zones of chaotic behavior in the parametrically excited pendulum. *J. Sound Vib.* **189**(1), 142-147.
 Brogliato, B. (1999) *Nonsmooth Mechanics*. Springer-Verlag, London.

- Bayly, P. V. And Virgin, L. N. (1992). Experimental evidence of diffusive dynamics and random walking in a single deterministic mechanical system: the shaken pendulum. *Int. J. Bifurcation and Chaos* 2(4), 983-988.
- Heng, H. Doerner, R. Hübinger, B. And Marfienssen, W. (1994). Approaching nonlinear dynamics by studying the motion of a pendulum, I: observing trajectories in state space. *Int. J. Bifurcation and Chaos* 4(4), 751-760.
- Müller, P. (1995). Calculation of Lyapunov exponents for dynamic systems with discontinuities. *Chaos, Solitons and Fractals* 5(9), 1971-1681.
- Skeledon, A. C. (1994). Dynamics of a parametrically excited double pendulum. *Physica D* 75, 541-558.
- Yagasaki, K. (1994) Chaos in a pendulum with feedback control. *Nonlin. Dyn.* 6, 125-142.
- Wolf, A. Swift, B. Swinney, H. And Vastano, J. (1985) Determining Lyapunov exponents from a time series. *Physica D* 16, 285-317.